International Agrophysics 5 (3–4), pp. 231–246 (1989)

BIOOPTICAL STUDY OF THE CORNEAL LENS OF THE WATER BUG *NOTONECTA GLAUCA*

G. HORVÁTH[1] and P. GREGUSS[2]

[1]*Hungarian Academy of Sciences, Central Research Institute for Physics, Biophysical Group P.O. Box 49, H–1525 Budapest, Hungary*

[2]*Applied Biophysics Laboratory, Institute of Precision Mechanics and Optics, Technical University of Budapest P.O. Box 91, H–1502 Budapest, Hungary*

(Received 31 August 1989)

A geometric optical calculation is given for the shape of the transition interface which eliminates longitudinal spherical aberration in the corneal lens of the backswimmer (*Notonecta glauca*). This interface is determined for differently-shaped corneal lenses. The advantage of the cornea of *Notonecta* is shown in comparison with other possible corneal lenses.

Keywords: biooptics, geometrical optics, corrected lens, spherical aberration.

Introduction

The approximate shape of the transition layer in the corneal lens of the water bug known as the backswimmer (*Notonecta glauca*) has already been calculated by Schwind [1, 2]. His calculations employed the radii of the circular arcs that closely approximate the refracting surfaces or the isorefraction line. Five circles were used for the interfacial curve between the two lens units. The computation was simplified by taking the regions between the best-approximation arcs as optically homogeneous. This approximate numerical method is difficult , slow and is not exact enough; it does not allow the quick determination of the exact theoretical shape of the transition layer for differently-shaped corneal lenses. Furthermore, the question: "what is the optimal shape of the corneal lens of the backswimmer?" is not yet made clear.

In this work we solve directly the geometric optical problem of the transition layer of the backswimmer. Using a general and exact method, we determine the shape of the transition layer for three differently-formed corneal lenses. On the basis of this investigation we then show the advantage of the real cornea of *Notonecta glauca* in comparison with other possible lenses.

Akadémiai Kiadó/Agroinform, Budapest
Kluwer Academic Publishers

The way of life of the backswimmer

The backswimmer is perfectly suited to life in water: it always swims upside down under water, and in a state of rest it hangs on the film of the water surface with its claws and periodically pushes up the tip of its abdomen to breathe.

The prey of *Notonecta glauca* are in general smaller insects which have fallen into the water, and certain tiny water animals. The backswimmer locates the position of prey which has fallen into the water on the basis of the ripples of the water surface produced by the prey. The bug senses these surface ripples with the scolopidial organ on its claws [3, 4].

Notonecta glauca behaves as an amphibian, it leaves the water if its environment becomes unsuitable or when it finds a partner for copulation. It can find a new body of water on the basis of the skylight reflected and polarized by the water surface [5, 6]. The optical localization technique of this predacious, amphibious bug is well-known. Schwind investigated experimentally the visual system, the dioptric apparatus of the backswimmer, and the way in which it exploits polarized light [1, 2, 5–7].

Backswimmers prefer turbid, still water with a dense growth of aquatic plants [8], their peripheral rhabdomeres serve as a scotopic system – they are used to perceive dim light in turbid water [9]. In that the diameter of the backswimmer's corneal lenses is small 40 μm, were the diameter to be smaller the lenses would not be suitable because in this case the amount of light that would be received by an individual cornea could be insufficient. The backswimmer's corneal lenses without longitudinal spherical aberration serve the purpose of increasing the light-collecting efficiency and the optimal high contrast, which both have relevance to the survival of the organism.

The eye of the backswimmer

The dioptric apparatus of the apposition eye of *Notonecta glauca* has two optically important properties. The entrance surface of the cornea is very flat, and it is almost perpendicular to the axis of the ommatidium [2]. The lens consists of two optically homogeneous units, and there is a bell-shaped thin transition layer between them, in which the refractive index varies continuously [1] (see Figs 1 and 2).

The amphibious manner of life is made possible for the backswimmer by the flat entrance surface of the cornea, with which the bug can see sharply in water as well as in air. In the insert of Fig. 2 the structure of an ommatidium of *Notonecta glauca* can be seen [1, 2]. Only those incident rays of light which are almost parallel to the axis of the ommatidium (called paraxial rays) take part in constructing the image because the other rays are absorbed in the pigment cells around the dioptric apparatus, and the rhabdom senses only the paraxial incident rays. This is typical in any apposition eye. Thus, the focus of the corneal lens does not change when the bug leaves the water.

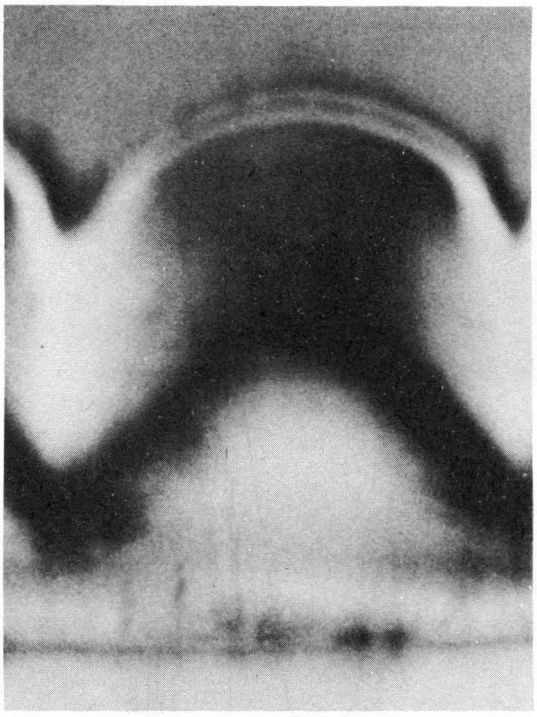

Fig. 1. Interference micrograph of a section through the corneal lens of a backswimmer (courtesy of Professor Schwind [2]). The diameter of the cornea is 40 *um*. The bell-shaped thin transition layer can be seen

The bell-shaped thin transition layer divides the cornea into two parts (see Fig. 2). Schwind showed experimentally that this layer eliminates the longitudinal spherical aberration of the cornea and yields an exact focal point on the distal tip of the crystalline cone (see Fig. 3) [2].

Calculation of the transition interface in differently-shaped corneal lenses

The thin transition layer in the cornea of the backswimmer is considered as an exact geometrical interface in our optical model. We place the corneal lens in the system of co-ordinates of Fig. 3, where the cross section of the dioptric apparatus, which has a radially symmetrical structure, can be seen. The shape of the entrance surface of the cornea, the

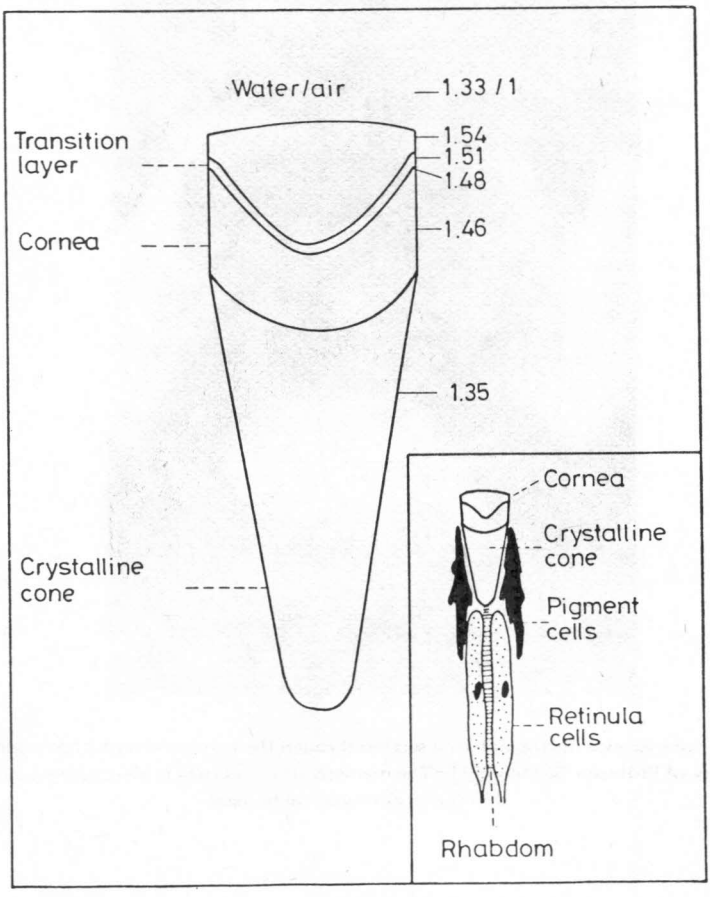

Fig. 2. The dioptric apparatus of the backswimmer consists of the corneal lens and the crystalline cone. The medium in contact with the entrance surface of the cornea is water or air. The numbers of the right side are the refractive indices. Insert: the structure of an ommatidium of the backswimmer

exit surface and the transition interface are described by the functions $f_1(x_1)$, $f_2(x_2)$ and $y(x)$ respetively. The numerical value of the geometrical parameters a, b, c, d, L, r of the dioptric apparatus and the refractive indices n_1, n_2, n_3, n_4 (see Fig. 3) are given in Table 1 for the cornea of *Notonecta glauca* [1, 2].

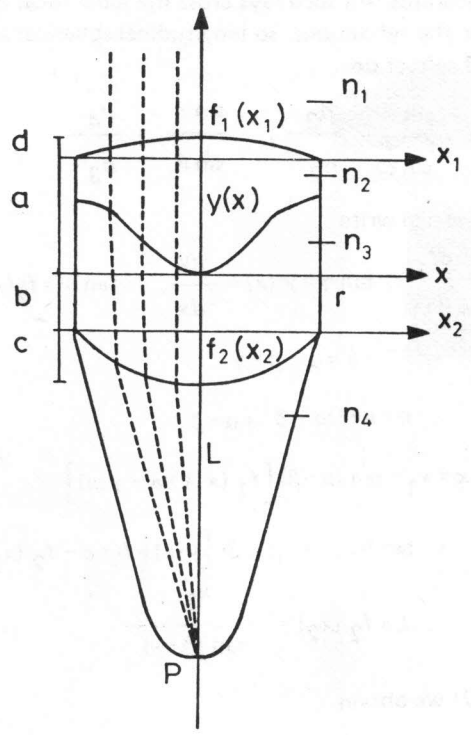

Fig. 3. Model of the dioptric apparatus of the backswimmer. Functions $f_1(x_1), f_2(x_2)$ and $y(x)$ describe (in main section) the entrance and the exit surface and the transition interface of the cornea, respectively. Focal point P is at distance L from the exit surface a, b, c, d and n_1, n_2, n_3, n_4 are the geometrical parameters and refractive indices

Table 1

Numerical value of the refractive indices and the geometrical parameters of the dioptric apparatus of *Notonecta glauca* [1, 2]

n_1(water) = 1.333, n_1 (air) = 1, n_2 = 1.54 n_3 = 1.46, n_4 = 1.35

L = 76 μm, r = 20 μm, a = 23 μm, b = 11 μm, c = 12 μm, d = 1 μm

Figure 4 shows the path of an incident ray of light parallel to the axis of the ommatidium in the dioptric apparatus. All such rays cross the same focal point P on the peak of the crystalline cone after the refractions, so longitudinal spherical aberration is eliminated. We can use the law of refraction

$$\frac{\sin\alpha}{\sin\beta} = \frac{n_2}{n_1}, \quad \frac{\sin\delta}{\sin\omega} = \frac{n_3}{n_2}, \quad \frac{\sin\eta}{\sin\theta} = \frac{n_4}{n_3} \tag{1}$$

On the basis of Fig. 4 we can write

$$\tan\alpha = -f_1'(x_1) \equiv -\frac{df_1}{dx_1}, \quad \tan\gamma = y'(x) \equiv \frac{dy}{dx}, \quad \tan\nu = f_2'(x_2) \equiv \frac{df_2}{dx_2} \tag{2}$$

$$\delta = \alpha - \beta + \gamma \tag{3}$$

$$\eta = \nu + \omega - \delta + \alpha - \beta \tag{4}$$

$$x = x_1 - \tan(\alpha-\beta)\left[f_1(x_1) + a - y(x)\right] \tag{5}$$

$$x_2 = x - \tan(\omega - \delta + \alpha - \beta)\left[y(x) + b + c - f_2(x_2)\right] \tag{6}$$

$$L + f_2(x_2) = \frac{x_2}{\tan(\theta-\nu)} \tag{7}$$

From equations (1) – (7) we obtain

$$\tan(\alpha-\beta) = \frac{-f_1'(x_1) + \dfrac{f_1'(x_1)\, n_1/n_2}{\left[1+f_1'^2(x_1)\right]^{1/2}}}{\left[1 - \dfrac{f_1'^2(x_1)\,(n_1/n_2)^2}{1+f_1'^2(x_1)}\right]^{1/2}} \Bigg/ \left[1 + f_1'^2(x_1)\right] \frac{n_1/n_2}{\left[1+f_1'^2(x_1)\right]^{1/2}} \Bigg/ \left[1 - \frac{f_1'^2(x_1)\,(n_1/n_2)^2}{1+f_1'^2(x_1)}\right]^{1/2} \tag{8}$$

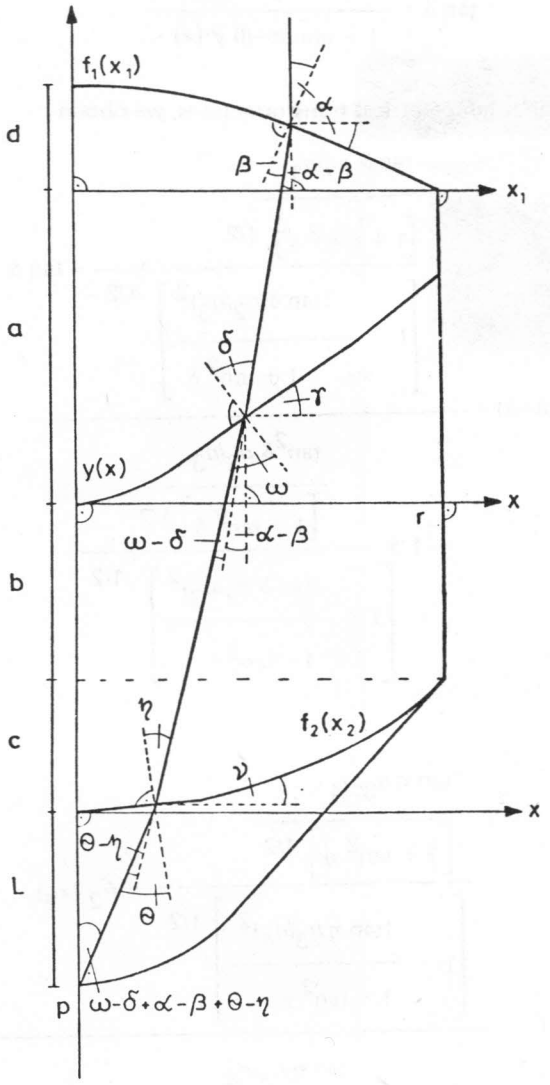

Fig. 4. Path of an incident ray of light parallel to the axis of the ommatidium in the dioptric apparatus of *Notonecta glauca*. Only half of the cross section is represented

From (2) and (3) we get

$$\tan \delta = \frac{\tan (\alpha - \beta) + y'(x)}{1 - \tan (\alpha - \beta)\, y'(x)} \tag{9}$$

Using (1) and some trigonometrical transformations, we obtain

$$\tan (\omega - \delta) = \frac{\dfrac{\tan \delta\, n_2/n_3}{\left[1 + \tan^2 \delta\right]^{1/2}} - \tan \delta}{\left[1 - \dfrac{(\tan \delta\, n_2/n_3)^2}{1 + \tan^2 \delta}\right]^{1/2}} \Bigg/ \frac{\dfrac{\tan^2 \delta\, n_2/n_3}{\left[1 + \tan^2 \delta\right]^{1/2}}}{\left[1 + \dfrac{(\tan \delta\, n_2/n_3)^2}{1 - \tan^2 \delta}\right]^{1/2}} \tag{10}$$

$$\tan (\theta - \nu) = \frac{\dfrac{\tan \eta\, n_3/n_4}{\left[1 + \tan^2 \eta\right]^{1/2}} - f'_2(x_2)}{\left[1 - \dfrac{(\tan \eta\, n_3/n_4)^2}{1 + \tan^2 \eta}\right]^{1/2}} \Bigg/ \frac{\dfrac{\tan \eta\, n_3/n_4}{\left[1 + \tan^2 \eta\right]^{1/2}}}{\left[1 - \dfrac{(\tan \eta\, n_3/n_4)^2}{1 + \tan^2 \eta}\right]^{1/2}} \tag{11}$$

$$1 + f'_2(x_2)$$

Using (2) and (4) we can write

$$\tan\eta = \frac{\tan(\omega - \delta + \alpha - \beta) + f'_2(x_2)}{1 - \tan(\omega - \delta + \alpha - \beta)\, f'_2(x_2)} \tag{12}$$

Equations (5) – (12) constitute a system of equations for calculating the shape of the transition interface in a lens without longitudinal spherical aberration. Then we apply this theory for differently-shaped lenses, and determine the interfacial curve $y(x)$. The following type of differential equation derives from the system of equations (5) – (12)

$$F[x, y(x), y'(x), f_1(x_1), f_2(x_2), a, b, c, d, L, n_1, n_2, n_3, n_4] = 0 \tag{13}$$

We consider three cases. In the case of a trapezoid corneal lens (see Fig. 5), functions $f_1(x_1)$ and $f_2(x_2)$ are

$$f_1(x_1) = d - x_1 d/r, \qquad f_2(x_2) = x_2 c/r \tag{14}$$

Substituting (14) into the system of equations (5) – (12) we obtain

$$z^4(Q_1 h_1 - k_1) + z^3(k_2 - Q_2 h_1 - Q_1 h_2) + z^2(h_2 Q_2 + h_1 Q_3 + Q_1 h_3 - k_3) -$$
$$-z(h_2 Q_3 + Q_2 h_3 - k_2) + Q_3 h_3 - k_4 = 0, \qquad z = \tan(\omega - \delta + \alpha - \beta) \tag{15}$$

$$\tan(\alpha - \beta) = \frac{d/r - \dfrac{n_1 d/(r n_2)}{\left[1 + d^2/r^2\right]^{1/2}}}{\left[1 - \dfrac{(d^2/r^2)(n_1/n_2)^2}{1 + d^2/r^2}\right]^{1/2}} \Bigg/ \left(1 + (d^2/r^2)\, \frac{n_1/n_2}{\left[1 + d^2/r^2\right]^{1/2}}\right) \Bigg/ \left[1 - \frac{(d^2/r^2)(n_1/n_2)^2}{1 + d^2/r^2}\right]^{1/2} \tag{16}$$

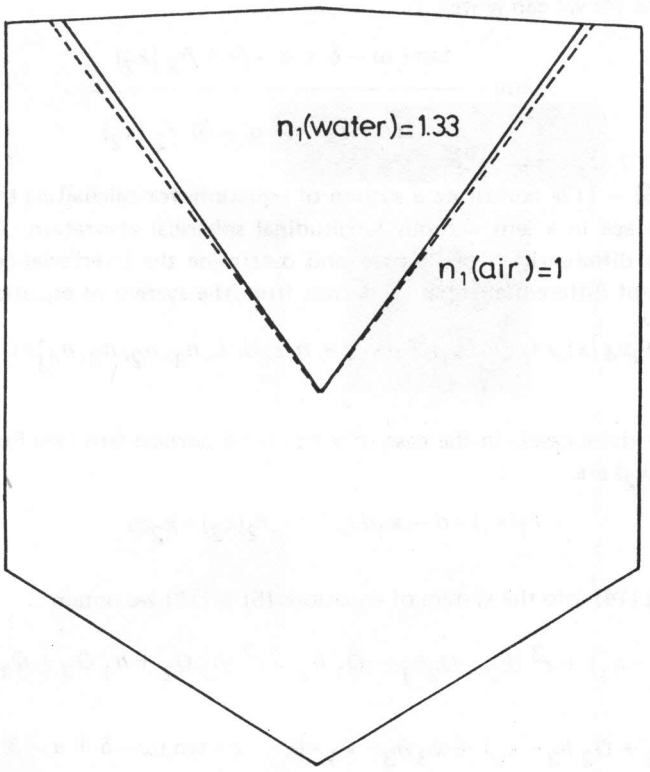

Fig. 5. Theoretically determined interfacial curve for water and air in a trapezoid corneal lens

$$\tan(\omega-\delta)=\frac{\tan(\omega-\delta+\alpha-\beta)-\tan(\alpha-\beta)}{1+\tan(\omega-\delta+\alpha-\beta)\tan(\alpha-\beta)} \tag{17}$$

$$\tan^4\delta\left\{1-(n_2/n_3)^2\left[1+\tan^2(\omega-\delta)\right]\right\}+2\tan^3\delta\tan(\omega-\delta)+$$
$$+2\tan^2\delta\left[1-(n_2/n_3)^2\right]\left[1+\tan^2(\omega-\delta)\right]+\tan\delta\tan(\omega-\delta)+ \tag{18}$$
$$+\tan^2(\omega-\delta)=0$$

$$y'(x)=\frac{\tan\delta-\tan(\alpha-\beta)}{1+\tan\delta\tan(\alpha-\beta)} \tag{19}$$

The notation used in (15) can be found in the Appendix (A(1)) Equations (15) and (18) are fourth degree equations for z and $\tan\delta$ respectively, and can therefore be solved analytically. Because of the extreme complexity of further analytical treatment, the numerical solution is quicker and simpler. During the numerical solution using the tangent method of Newton, we solved (15) for z, then using (16), (17) we solved (18) for $\tan\delta$, then using (16) obtained $y'(x)$ from (19). From here the function $y(x)$ can be determined, using the iteration $y(x+\Delta x) = y(x) + y'(x) \cdot \Delta x$; $\Delta x = r/m$, where m is a large number ($m \gg 1$). We determined $y(x)$ for n_1 (water) = 1.333 and n_1 (air) = 1, the curves obtained are shown in Fig. 5.

If we substitute $c=d=0$ into the above expressions obtained for a trapezoid lens, we then obtain the case of the plane-parallel lens

$$z^4 (y+b)^2 A - 2z^3 x(y+b) A + z^2 \left[x^2 A + (y+b)^2 - (Ln_3/n_4)^2\right] - \\ - 2zx(y+b) + x^2 = 0, \qquad A = 1 - (n_3/n_4)^2 \tag{20}$$

$$y'^4 \left[1 - B(1+z^2)\right] + 2zy'^3 + y'^2 (1-B)(1+z^2) + 2zy' + z^2 = 0 \\ B = (n_2/n_3)^2 \tag{21}$$

We also solved numerically (20) for z, then (21) for $y'(x)$. After this we obtained the interfacial curve $y(x)$. The result is given in Fig. 6. The paraxial incident rays of light do not refract on the entrance surface of the plane-parallel lens, so the shape of the interfacial curve $y(x)$ is independent of the refractive index n_1.

The shape of the cornea of the backswimmer can be approached by a plane-paraboloid lens [1, 2]

$$f_1(x_1) = 0, \qquad f_2(x_2) = c(x_2/r)^2 \tag{22}$$

Substituting (22) into the system of equations (5) – (12) we obtain

$$P_{12} x_2^{12} + P_{10} x_2^{10} - P_9 x_2^9 + P_8 x_2^8 + P_7 x_2^7 + P_6 x_2^6 - P_5 x_2^5 + P_4 x_2^4 + P_3 x_2^3 \\ + P_2 x_2^2 - P_1 x_2 - P_0 = 0 \tag{23}$$

$$y'^4 \left[1 - \frac{n_2^2}{n_3^2}(1+z^2)\right] + 2zy'^3 + y'^2 \left(1 - \frac{n_2^2}{n_3^2}\right)(1+z^2) + 2zy' + z^2 = 0 \tag{24}$$

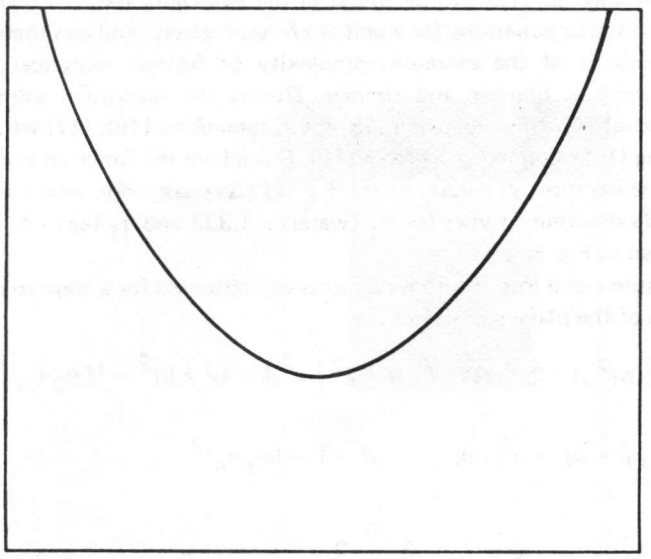

Fig. 6. Theoretically determined interfacial curve in a plane-parallel corneal lens

The notation used in (23) and (24) can be found in the Appendix (A(2)). We solved (23), (24) numerically (using the tangent method of Newton). During the solution the refractive index n_1 can be optional, similar to the case of the plane-parallel lens. The result is shown in Fig. 7.

Conclusion

The theoretical transition interfaces in the trapezoid (cornea A) and plane-parallel (cornea B) lenses cross the entrance surface of the cornea (see Figs 5 and 6) for the parameters presented in Table 1, therefore the interface cannot eliminate the longitudinal spherical aberration for the whole of the diameter of the lens. So the diameter of the spherically-corrected lens is smaller than 40 μm for corneas A and B. The theoretical transition interface in the plane-paraboloid (cornea *C*) lens is flatter than in corneas A and B (see Fig. 7), and it can eliminate the spherical aberration for the whole diameter of 40 μm.

The light-collecting efficiency of a lens is proportional to $(r/f)^2$. Focal length f is equal for corneal lenses A, B and C investigated, but $r < 40$ μm in corneas A, B, and $r = 40$ μm in cornea C. Thus, the light-collecting efficiency of the plane-paraboloid cornea investigated is greater than that of the other two lenses considered, therefore the former lens is optimal among the above three lenses.

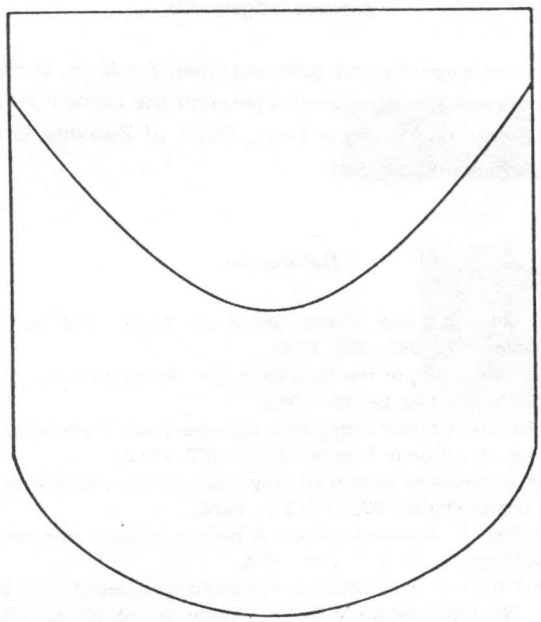

Fig. 7. Theoretically determined interfacial curve in a plane-paraboloid corneal lens

Spherical aberration becomes important when the size of the blur circle is larger than the diameter of the Airy disk due to diffraction, which is given by

$$d = 2.44 f\lambda/(nD) \tag{25}$$

where λ, f, D and n are the wavelength of the ray of light, the focal length, the diameter and the refractive index of the lens, respectively [2, 10, 11]. Whereas the diameter of the diffraction disk decreases with increasing relative aperture, the diameter of the blur circle increases, approximately as the cube of D/f. The intersections of these two curves show that spherical aberration is not important in very small lenses. Since the diameter of the corneal lenses of the backswimmer is quite small, the advantages which accrue from correcting for spherical aberration are not large. On the other hand Schwind showed [2] that the value of the frequency-response curve is 28% higher for the spherically-corrected corneal lens than it is for the uncorrected lens, which has a wave from aberration of $A \approx 1$ at $\lambda = 546$ nm.

The structure of the large corneal lenses of several trilobites that died out 400–500 million years ago is quite similar to that of *Notonecta glauca* [12].

Acknowledgements

Thanks are due to Professor Rudolf Schwind (Inst. Zoologie, Univ. Regensburg, FRG) for the interference micrograph of a section through the corneal lens of a backswimmer and to Dr. Gábor Bakonyi (Agricultural Univ., Dept. of Zoology, Gödöllő, Hungary) for his continuous advice, help and support.

References

1. Schwind, R.: Sehen unter und über Wasser, Sehen von Wasser, Das Sehsystem eines Wasserinsectes. Naturwissenschaften 72, 343–352. 1985.
2. Schwind, R.: Geometrical optics of the *Notonecta eye:* Adaptations to optical environment and way of life. J. Comp. Physiol. 140, 59–68. 1980.
3. Wiese, K.: Das mechanorezeptorische Beuteortungssystem von *Notonecta*, I. Die Funktion des tarsalen Scolopidialorgans. J. Comp. Physiol. 78, 83–102. 1972.
4. Wiese, K.: The mechanoreceptive system of prey localization in *Notonecta*, II. The principle of prey localization. J. Comp. Physiol. 92, 317–325. 1974.
5. Schwind, R.: Visual system of *Notonecta glauca*: A neuron sensitive to movement in the binocular visual field. J. Comp. Physiol. 123, 315–328. 1978.
6. Schwind, R.: Evidence for true polarization vision based on a two-channel analyzer system in the eye of the water bug, *Notonecta glauca*. J. Comp. Physiol. A 154, 53–57. 1984.
7. Schwind, R.: Zonation of the optical environment and zonation in the rhabdom structure within the eye of the backswimmer, *Notonecta glauca* . Cell Tissue Res., 232, 53–63. 1983
8. Giller, P. and McNeill, S.: Predation strategies, resource partitioning and habitat selection in *Notonecta*. J. Animal Ecol. 50, 798–808. 1981.
9. Schwind, R., Schlecht, P. and Langer, H.: Microspectrophotometric characterization and localization of three visual pigments in the compound eye of *Notonecta glauca*. J. Comp. Physiol. A 154, 341–350. 1984.
10. Vogt, K.: Optische Untersuchungen an der Cornea der Mehlmotte Ephestia kühniella. J. Comp. Physiol. 88, 201–216. 1974.
11. Land, M.F.: Handbook of Sensory Physiology VII/6B, ed.: Autrum, H, Berlin, Springer, 1981.
12. Clarkson, E.N.K., Levi-Setti, R.: Trilobite eyes and the optics of Des Cartes and Huygens. Nature 254, 663–667. 1975.

APPENDIX

The notation used in (15)

$$k_1 = (n_3 Lc/n_4 r)^2 \ , \quad k_2 = 2c(1-c^2/r^2)\ (n_3 L/n_4)^2/r$$

$$k_3 = (n_3 L/n_4)^2\ (1 + c^4/r^4 - 4c^2/r^2) \ , \quad k_4 = (n_3 Lc/n_4 r)^2$$

$$h_1 = (c/r)^2 + 1 - (n_3^2/n_4^2)^2 \ , \quad h_2 = 2c(n_3/n_4)^2/r$$

$$h_3 = 1 + (c/r)^2\ (1 - n_3/n_4)$$

$$Q_1 = L^2 c^4/r^4 + (1 + c^2/r^2)\ (y + b + c)\left[2Lc^2/r^2 + (1 + c^2/r^2)\ (y + b + c)\right]$$

$$Q_2 = 2L^2\ (c/r)^3 + 2\ (1 + c^2/r^2)\ (y + b + c)\left[Lc/r + x(1 + c^2/r^2)\right] +$$

$$+ 2L\ (c/r)^2\ (1 + c^2/r^2)\ x$$

$$Q_3 = (Lc/r)^2 + x\ (1 + c^2/r^2)\left[2Lc/r + x(1 + c^2/r^2)\right] \qquad \text{A(1)}$$

The notation used in (23) and (24)

$$k_1 = 1 + 4c^2 L^2/r^4 + 4cL/r^2 \ , \quad k_2 = 4c^4/r^8 \ , \quad k_3 = 4c^2/r^4 + 8c^3 L/r^6$$

$$g_1 = (n_3 L/n_4)^2 \ , \quad g_2 = (n_3 c/n_4 r^2)^2 - (1 - n_3^2/n_4^2)\, k_3$$

$$g_3 = 2cL\ (n_3/n_4 r)^2 + (1 - n_3^2/n_4^2)\, k_1 \ , \quad g_4 = (1 - n_3^2/n_4^2)\, k_2$$

$$h_1 = 4cx\ (y + b + c)\ /\ r^2 - 2x \ , \quad h_2 = 1 + 4c^2\ (y + b + c)^2\ /\ r^4 - 4c\ (y + b + c)\ /\ r^2$$

$$h_3 = 4c^2 / r^4 - 8c^3 (y + b + c) / r^6 , \quad h_4 = 4c^4 / r^8 , \quad h_5 = 4c^2 x / r^4$$

$$Q_1 = 4c^2 x / r^4 , \quad Q_2 = (y + b + c)^2 , \quad Q_3 = c^2 / r^4$$

$$Q_4 = 2c(y + b + c) / r^2 + 4c^2 x^2 / r^4 , \quad Q_5 = 4cx(y + b + c) / r^2$$

$$P_{12} = h_4 g_4 , \quad P_{10} = Q_3 k_2 - h_4 g_2 + h_3 g_4 , \quad P_9 = Q_1 k_2 + h_5 g_4$$

$$P_8 = Q_3 k_3 + Q_4 k_2 - h_3 g_2 + h_4 g_3 + h_2 g_4 , \quad P_7 = h_5 g_2 + h_1 g_4 - Q_1 k_3 - Q_5 k_2$$

$$P_6 = Q_4 k_3 + Q_2 k_2 + Q_3 k_1 - h_2 g_2 - h_4 g_1 + h_3 g_3 + x^2 g_4$$

$$P_5 = h_1 g_2 + h_5 g_3 + Q_5 k_3 + Q_1 k_1 , \quad P_4 = Q_2 k_3 + Q_4 k_1 - h_3 g_1 - x^2 g_2 + h_2 g_3$$

$$P_3 = h_1 g_3 + h_5 g_1 - Q_5 k_1 , \quad P_2 = Q_2 k_1 - h_2 g_1 + x^2 g_3 , \quad P_1 = h_1 g_1 , \quad P_0 = x^2 g_1$$

$$z = \tan (\omega - \delta) = \frac{x - x_2}{y + b + c - c (x_2 / r)^2} \qquad \text{A(2)}$$